

ORIGINAL
RESEARCH

Y. Liu
A. Aeby
D. Balériaux
P. David
J. Absil
V. De Maertelaer
P. Van Bogaert
F. Avni
T. Metens



White Matter Abnormalities Are Related to Microstructural Changes in Preterm Neonates at Term-Equivalent Age: A Diffusion Tensor Imaging and Probabilistic Tractography Study

BACKGROUND AND PURPOSE: Preterm infants have a high risk of brain injury and neurodevelopmental impairment, often associated with WMA on conventional MR imaging. DTI can provide insight into white matter microstructure. The aim of this study was to investigate the association between WMA on conventional MR imaging and DTI parameters in specific fibers in preterm neonates at term-equivalent age.

MATERIALS AND METHODS: Seventy preterm neonates (39 boys and 31 girls) were included in the study. WMA were classified as no, mild, moderate, or severe. Probabilistic tractography provided tract volumes, FA, MD, $\lambda_{//}$, and λ_{\perp} in the CST, SLF, TRs, and corpus callosum. Data were compared by using MANOVA, and adjustment for multiple comparisons was performed.

RESULTS: Important associations were found between WMA and microstructural changes. Compared with neonates with no WMA ($n = 41$), those with mild WMA ($n = 27$) had significantly increased λ_{\perp} and MD in the left ATR, the left sensory STR, the bilateral motor STR, and for λ_{\perp} also in the right CST; FA decreased significantly in the left sensory STR. Diminished tract volumes and altered diffusion indices were also observed in the 2 neonates with moderate WMA.

CONCLUSIONS: Altered DTI indices in specific tracts, with λ_{\perp} as most prominent, are associated with mild WMA in preterm neonates at term-equivalent age.

ABBREVIATIONS: ATR = anterior thalamic radiation; CST = corticospinal tract; $\lambda_{//}$ = longitudinal diffusivity; λ_{\perp} = transverse diffusivity; MANOVA = multivariate analysis of variance; MD = mean diffusivity; pre-OL = pre- and immature oligodendroglial cells; PTR = posterior thalamic radiation; SLF = superior longitudinal fasciculus; STR = superior thalamic radiation; TRs = thalamic radiations; WMA = white matter abnormalities

The incidence of preterm birth is increasing and accounts for 5%–13% in industrialized countries.¹ Preterm infants are at high risk of brain injury and poor neurodevelopmental outcome. Motor disabilities are typical, with approximately 2%–7% of preterm infants developing cerebral palsy,² usually associated with cystic periventricular leucomalacia on MR imaging.^{3–5} Cognitive, behavioral, and social difficulties are more common than motor dysfunction^{6,7}; however, their correlation with imaging is still debated. They may be associated with subtle WMA—for example, diffuse excessive high signal intensity on T2-weighted images⁸ and other abnormal T1 or T2 signals.^{9,10} Woodward et al¹¹ have shown that WMA on conventional MR imaging at term-equivalent age (gestational age

of 40 weeks) predict adverse neurodevelopmental outcomes at 2 years of age in preterm infants. However, the evaluation of conventional MR imaging is limited in qualitative assessments, and it does not provide information on the extent of the injury in specific white matter pathways.

DTI is currently the best noninvasive technique to assess microstructural changes in white matter pathways. DTI enables quantitative assessment of brain normal structures and lesions by calculating FA, MD, $\lambda_{//}$, and λ_{\perp} . FA expresses the fraction of anisotropic diffusion. MD corresponds to the directionally averaged magnitude of water diffusion. $\lambda_{//}$ expresses the parallel diffusion to white matter fibers; a marked decrease of $\lambda_{//}$ reflects axonal injury.¹² λ_{\perp} expresses the perpendicular diffusion to the fiber direction; an increase of λ_{\perp} indicates reduced oligodendroglial integrity around the axons.¹²

Fiber tracking allows the visualization of white matter tracts. Previous studies have showed significant region-specific changes in diffusion indices in preterm infants with WMA at term-equivalent age.^{13–15} However, the diffusion indices of these studies were obtained from predefined ROIs in white matter but not in specific fiber tracts. Only a few studies have used DTI and tractography for the assessment of white matter injury in neonates,^{16,17} and most tractography studies were performed on children older than 2 years of age and usually in a small cohort.^{18–20} Little is known about the microstructural changes in specific fiber tracts in the preterm brain

Received June 28, 2011; accepted after revision August 3.

From the Departments of Radiology (Y.L., D.B., P.D., J.A., F.A., T.M.) and Pediatric Neurology (A.A., P.V.B.), and Laboratoire de Cartographie Fonctionnelle du Cerveau (A.A., P.V.B.), ULB-Hôpital Erasme, Brussels, Belgium; and Institut de Recherche Interdisciplinaire en Biologie Humaine et Moléculaire and Department of Biostatistics and Medical Informatics (V.D.M.), ULB, Brussels, Belgium.

This work was supported by grants from the Fonds Xénophilia (ULB), and the Fond de la Recherche Scientifique of Belgium (project grant No. 1.5.149.10).

Please address correspondence to Yan Liu, MD, Department of Radiology, ULB-Hôpital Erasme, 808 Lennik St, 1070 Brussels, Belgium; e-mail address: yanliu@ulb.ac.be



Indicates open access to non-subscribers at www.ajnr.org



Indicates article with supplemental on-line tables.

<http://dx.doi.org/10.3174/ajnr.A2872>

Table 1: WMA assessment at conventional MRI			
Characteristics	Score 1	Score 2	Score 3
White matter signal abnormality	Normal 34/70 (48.6%)	Focal regions (<2 regions per hemisphere) 15/70 (21.4%)	Multiple regions (>2 regions) 21/70 (30.0%)
White matter volume loss	Normal 61/70 (87.1%)	Mild reduction with increased ventricular size (EI = 0.3–0.36) 9/70 (12.9%)	Marked reduction with increased ventricular size (EI > 0.36) 0/70 (0%)
Cystic abnormalities	Normal 66/70 (94.3%)	<2-mm single focal cyst 0/70 (0%)	Multiple cysts or a single larger (>2 mm) focal cyst 4/70 (5.7%)
Ventricular dilation	Normal 57/70 (81.4%)	Mild-moderate enlargement of the frontal, temporal, and occipital horns 12/70 (17.2%)	More global enlargement of the frontal, temporal, and occipital horns 1/70 (1.4%)
Thinning of the corpus callosum	Normal 54/70 (77.2%)	Focal thinning in the corpus callosum 15/70 (21.4%)	Global thinning across the entire corpus callosum 1/70 (1.4%)

Note:—EI indicates Evans Index.

at term-equivalent age, and to our knowledge, no study has yet shown the association between microstructural changes by fiber tracking and WMA graded according to Woodward et al.¹¹

In this study by using DTI and probabilistic tractography, we investigated DTI parameters (tract volume, FA, MD, $\lambda_{//}$, and λ_{\perp}) in the CST, SLF, TRs, and corpus callosum. The aim of the study was to investigate whether WMA on conventional brain MR imaging are related to diffusion changes in specific fiber tracts.

Materials and Methods

Patients

During a 5-year period (from October 2005 to September 2010) in our institution, 301 preterm neonates underwent brain MR imaging without sedation for detecting lesions related to premature birth.¹¹ Two hundred twenty-six neonates were excluded from the study due to the movement artifacts on conventional MR imaging or on DTI. Furthermore, we excluded 3 neonates with known malformations or

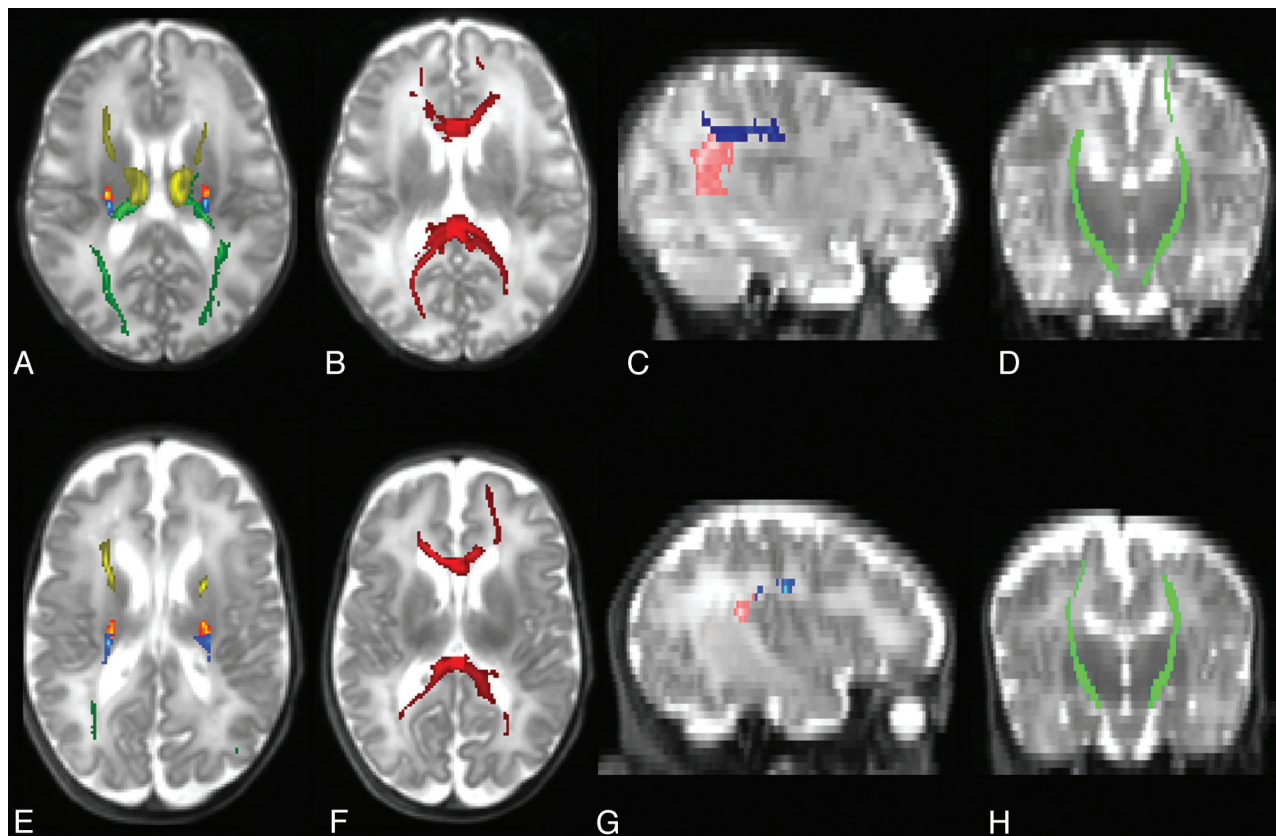


Fig 1. Tracts are shown on T2-weighted images in neonate with no WMA, scanned at 36 weeks corrected gestational age (A–D) and in neonate with moderate WMA, scanned at 38 weeks (E–H). Axial images (A, E) show the TRs (ATR in yellow, motor STR in yellow-red, sensory STR in blue and PTR in dark green). Axial images (B, F) show the corpus callosum (dark red). Sagittal images (C, G) show the frontoparietal SLF (dark blue) and parietotemporal SLF (pink). Coronal (D, H) images show the CSTs (light green). Images were obtained from a 1.5T magnet (Philips Achieva, Best, The Netherlands).

	Preterm with No WMA (n = 41) (mean) (SD)	Preterm with Mild WMA (n = 27) (mean) (SD)	P Value	Preterm with Moderate WMA (n = 2)
CST (left)	0.28 (0.03)	0.27 (0.04)	.022	Case 1: 0.25 Case 2: 0.21
CST (right)	0.28 (0.04)	0.26 (0.04)	.005	Case 1: 0.22 Case 2: 0.27
Frontoparietal SLF (left)	0.17 (0.03)	0.16 (0.03)	.020	Case 1: 0.12 Case 2: 0.13
Frontoparietal SLF (right)	0.18 (0.02)	0.16 (0.03)	.004	Case 1: 0.11 Case 2: 0.15
Parietotemporal SLF (left)	0.17 (0.02)	0.16 (0.03)	.077	Case 1: 0.09 Case 2: 0.14
Parietotemporal SLF (right)	0.16 (0.02)	0.15 (0.03)	.191	Case 1: 0.11 Case 2: 0.14
ATR (left)	0.19 (0.02)	0.18 (0.03)	.012	Case 1: 0.16 Case 2: 0.16
ATR (right)	0.19 (0.02)	0.18 (0.03)	.045	Case 1: 0.12 Case 2: 0.17
Motor STR (left)	0.25 (0.03)	0.23 (0.04)	.005	Case 1: 0.22 Case 2: 0.20
Motor STR (right)	0.25 (0.03)	0.24 (0.05)	.024	Case 1: 0.19 Case 2: 0.24
Sensory STR (left)	0.24 (0.03)	0.22 (0.03)	<.001 ^a	Case 1: 0.15 Case 2: 0.17
Sensory STR (right)	0.23 (0.02)	0.22 (0.04)	.006	Case 1: 0.17 Case 2: 0.18
PTR (left)	0.21 (0.03)	0.20 (0.03)	.103	Case 1: 0.09 Case 2: 0.15
PTR (right)	0.21 (0.02)	0.20 (0.03)	.009	Case 1: 0.11 Case 2: 0.17
Corpus callosum	0.26 (0.03)	0.24 (0.03)	.016	Case 1: 0.14 Case 2: 0.18

^a The *P* value reaches statistical significance after controlling for false discovery rate (*P* < .003).

congenital infections: 1 infant with Chiari type III, 1 with polymicrogyria, and 1 with congenital cytomegalovirus infection. Finally, 72 preterm neonates with applicable DTI sequences and conventional MR imaging were studied.

The study was approved by the ethics committee of our institution (Reference: P2004/207 and P2009/234), and informed written parental consent was obtained for each participant.

MR Imaging Data Acquisition

MR imaging examinations were performed with a 1.5T magnet (Achieva; Philips Healthcare, Best, the Netherlands) equipped with an 8-channel sensitivity encoding head coil. The following sequences were acquired for all subjects: 1) sagittal 3D T1-weighted gradient-echo images, 2) coronal and axial T2-weighted turbo spin-echo images, 3) axial inversion recovery images, 4) axial T2*-weighted gradient-echo images, and 5) spin-echo EPI images. For DTI acquisitions, we used the following parameters: TR/TE, 5888/92 ms; FOV, 220 × 220 mm; 32 noncollinear diffusion-sensitizing gradient directions with a diffusion sensitivity of *b* = 600 s/mm² and a 2 × 2 mm² in-plane resolution; acceleration factor (sensitivity encoding), 2.2; section thickness, 2.3 mm; and scanning time, 3 minutes 40 seconds.

No sedation was used; neonates were spontaneously asleep, positioned in a vacuum immobilization pillow to minimize body and head movements. Ear muffs were placed to minimize noise exposure. Oxygen saturation and electrocardiography were monitored throughout the acquisition.

	Preterm with No WMA (n = 41) (mean) (SD)	Preterm with Mild MWA (n = 27) (mean) (SD)	P Value	Preterm with Moderate WMA (n = 2)
CST (left)	1.340 (0.10)	1.362 (0.09)	.027	Case 1: 1.45 Case 2: 1.45
CST (right)	1.338 (0.09)	1.377 (0.12)	.005	Case 1: 1.45 Case 2: 1.34
Frontoparietal SLF (left)	1.45 (0.10)	1.45 (0.12)	.458	Case 1: 1.57 Case 2: 1.51
Frontoparietal SLF (right)	1.43 (0.10)	1.46 (0.12)	.071	Case 1: 1.53 Case 2: 1.43
Parietotemporal SLF (left)	1.48 (0.07)	1.48 (0.09)	.634	Case 1: 1.57 Case 2: 1.51
Parietotemporal SLF (right)	1.50 (0.11)	1.49 (0.09)	.879	Case 1: 1.51 Case 2: 1.45
ATR (left)	1.33 (0.07)	1.36 (0.09)	.003 ^a	Case 1: 1.47 Case 2: 1.44
ATR (right)	1.33 (0.07)	1.35 (0.09)	.045	Case 1: 1.54 Case 2: 1.36
Motor STR (left)	1.31 (0.10)	1.36 (0.10)	.001 ^a	Case 1: 1.45 Case 2: 1.47
Motor STR (right)	1.31 (0.10)	1.37 (0.14)	.002 ^a	Case 1: 1.43 Case 2: 1.32
Sensory STR (left)	1.32 (0.08)	1.37 (0.11)	.001 ^a	Case 1: 1.48 Case 2: 1.51
Sensory STR (right)	1.33 (0.10)	1.38 (0.11)	.012	Case 1: 1.50 Case 2: 1.40
PTR (left)	1.48 (0.08)	1.51 (0.10)	.064	Case 1: 1.57 Case 2: 1.60
PTR (right)	1.49 (0.08)	1.52 (0.09)	.047	Case 1: 1.51 Case 2: 1.54
Corpus callosum	1.57 (0.06)	1.59 (0.08)	.036	Case 1: 1.92 Case 2: 1.63

^a The *P* value reaches statistical significance after controlling for false discovery rate (*P* < .003).

Assessment of White Matter Injury

Two readers, experienced neuroradiologists (D.B. and P.D.), interpreted conventional MR imaging (sequences 1–4), blinded to the subject's clinical condition but informed of the subject's gestational age at birth and corrected gestational age at MR imaging.

WMA were graded according to Woodward et al,¹¹ by using 5 characteristics, each with a score of 1 (normal), 2 (mild abnormality), and 3 (moderate-severe abnormality) (Table 1). These 5 assessments of the cerebral white matter were then combined to give an overall WMA score, which was categorized in 4 groups: no abnormality (total score, 5–6), mild abnormality (total score, 7–9), moderate abnormality (total score, 10–12), and severe abnormality (total score, 13–15). In Table 1, the ventricular dilation was assessed by using the Evans Index, defined as the maximal frontal horn ventricular width divided by the transverse inner diameter of the skull.²¹

Disagreements on classification were resolved by consensus, and cases with unresolved discrepancies at consensus were excluded from further analysis.

Data Postprocessing

Data analysis was performed by using the software FSL (<http://www.fmrib.ox.ac.uk/fsl>).²²

Image Preparation

Image artifacts due to eddy current distortions and head movements were minimized by registering the DTI from 32 directions to the B0

Table 4: λ_{\perp} (10^{-3} mm²/s) in each tract

	Preterm with No WMA (n = 41) (mean) (SD)	Preterm with Mild WMA (n = 27) (mean) (SD)	P Value	Preterm with Moderate WMA (n = 2)
CST (left)	1.14 (0.10)	1.17 (0.12)	.007	Case 1: 1.29 Case 2: 1.29
CST (right)	1.14 (0.10)	1.19 (0.13)	.001 ^a	Case 1: 1.28 Case 2: 1.16
Frontoparietal SLF (left)	1.33 (0.11)	1.34 (0.13)	.291	Case 1: 1.48 Case 2: 1.41
Frontoparietal SLF (right)	1.31 (0.10)	1.35 (0.13)	.033	Case 1: 1.45 Case 2: 1.32
Parietotemporal SLF (left)	1.35 (0.07)	1.36 (0.10)	.403	Case 1: 1.50 Case 2: 1.40
Parietotemporal SLF (right)	1.38 (0.11)	1.38 (0.10)	.724	Case 1: 1.43 Case 2: 1.36
ATR (left)	1.20 (0.07)	1.23 (0.07)	.001 ^a	Case 1: 1.35 Case 2: 1.33
ATR (right)	1.20 (0.07)	1.23 (0.09)	.025	Case 1: 1.45 Case 2: 1.24
Motor STR (left)	1.14 (0.10)	1.20 (0.12)	<.001 ^a	Case 1: 1.31 Case 2: 1.32
Motor STR (right)	1.15 (0.10)	1.21 (0.15)	.001 ^a	Case 1: 1.29 Case 2: 1.18
Sensory STR (left)	1.16 (0.09)	1.22 (0.12)	<.001 ^a	Case 1: 1.37 Case 2: 1.38
Sensory STR (right)	1.18 (0.10)	1.23 (0.12)	.005	Case 1: 1.37 Case 2: 1.27
PTR (left)	1.32 (0.09)	1.36 (0.12)	.060	Case 1: 1.50 Case 2: 1.48
PTR (right)	1.33 (0.08)	1.36 (0.10)	.018	Case 1: 1.43 Case 2: 1.42
Corpus callosum	1.35 (0.07)	1.39 (0.09)	.012	Case 1: 1.79 Case 2: 1.63

^a The *P* value reaches statistical significance after controlling for false discovery rate (*P* < .003).

images.¹⁹ Maps of the diffusion indices were obtained by using FSL Diffusion Toolbox.²³

Probabilistic Tractography

The bundles were reconstructed in each subject by 1 investigator (Y.L.) by using multitensor probabilistic tractography.^{24,25} The masks were identified and manually placed by 2 neuroradiologists (Y.L. and D.B.) in consensus for each tract. The CST was tracked by using a seed mask in the cerebral peduncle and a waypoint mask in the precentral gyrus.²⁶ The SLFs were tracked separately into 2 parts^{27,28}: the frontoparietal SLF and the parietotemporal SLF. For the frontoparietal SLF, a seed mask covered the frontal white matter and the waypoint mask covered the frontoparietal white matter on coronal sections; for the parietotemporal SLF, the seed mask was the same as the waypoint mask of the frontoparietal SLF, and the waypoint mask covered the temporal lobe on an axial section.²⁷ The TRs were studied separately in 4 subradiations²⁷: ATR, the motor and sensory STR, and the PTR. A seed mask was positioned in the bottom of the thalamus, and a waypoint mask, in the anterior limb of the internal capsule for the ATR, in the precentral gyrus for the motor STR, in the postcentral gyrus for the sensory STR, and in the occipital lobe for the PTR. The corpus callosum was tracked by symmetric seed masks drawn on either side of the midline.¹⁹

The original tracts were normalized by the total number of samples going from the seed ROI to the target ROI.²⁵ Finally, the obtained

connectivity distributions were thresholded with a probability of 0.2% for the corpus callosum and 2% for the bilateral tracts.^{27,29,30}

The tract volume and diffusion indices (FA, MD, $\lambda_{//}$, and λ_{\perp}) of each tract were evaluated by using FSL calculations.²⁷

Statistical Analyses

All statistical analyses were performed with the Statistical Package for the Social Sciences, Version 15 (SPSS, Chicago, Illinois). A 1-sample Kolmogorov-Smirnov test was performed to detect a possible departure from normality of our variables. A MANOVA was used to compare tract volumes and diffusion indices between WMA groups; the corrected gestational age at MR imaging was considered as a covariate. After controlling for false discovery rate,³¹ statistical significance was reached when *P* < .003.

Results

Of the 72 preterm neonates who were recruited, 2 were excluded due to disagreement between readers on the conventional MR imaging assessment. Seventy neonates were included in the tractography study, and their clinical characteristics collected from patient medical records are given in On-line Table 1. Forty-one neonates were classified as having no WMA; 27 neonates, with mild WMA; 2 neonates, with moderate WMA; and no neonate, with severe WMA. Because of the small sample size (*n* = 2) of the moderate group, statistical analyses were only performed between the groups with no WMA and with mild WMA.

Clinical Characteristics

There were no significant differences in any of the clinical characteristics between the neonates with no and with mild WMA (data not shown).

Tract Volume in Relation to WMA

Tract volume results are detailed in On-line Table 2. No significant differences were found in tract volume between neonates with no WMA and with mild WMA. In case 1 with moderate WMA, showing diffuse white matter signal-intensity abnormalities, multiple cystic lesions, and thinning of the corpus callosum, some tract volumes were relatively small compared with the mean volumes in the neonates with no WMA (Fig 1). Case 2, showing diffuse white matter signal-intensity abnormalities and ventricular dilation, had no obviously decreased tract volume.

FA in Relation to WMA

Neonates with mild WMA had significantly lower FA in the left sensory STR compared with neonates with no WMA; in the 2 neonates with moderate WMA, we observed decreased FA values in the CST, SLF, TRs, and corpus callosum (Table 2).

MD in Relation to WMA

Neonates with mild WMA had significantly higher MD in the left ATR, the left sensory STR, and the bilateral motor STR compared with neonates with no WMA; in the 2 neonates with moderate WMA, we observed increased MD values in the CST, SLF, TRs, and corpus callosum (Table 3).

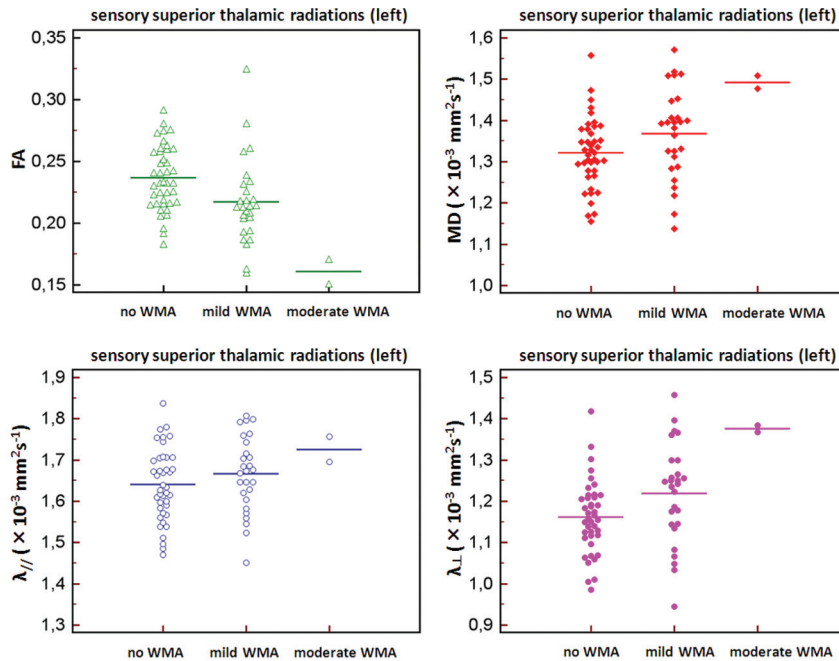


Fig 2. The diffusion indices in the left sensory STR are shown by scatter plots with mean (line) in neonates with no WMA, mild WMA and moderate WMA. Statistically significant differences (taking into account the gestational age as a covariate and after controlling for false discovery rate) were found for FA ($P < .001$), MD ($P = .001$), and λ_{\perp} ($P < .001$).

$\lambda_{//}$ in Relation to WMA

No significant differences in $\lambda_{//}$ were found between the neonates with no and mild WMA; in the 2 neonates with moderate WMA, no obvious changes were observed in $\lambda_{//}$ (On-line Table 3).

λ_{\perp} in Relation to WMA

Neonates with mild WMA had significantly higher λ_{\perp} in the left ATR, the left sensory STR, the bilateral motor STR, and the right CST compared with neonates with no WMA; in 2 neonates with moderate WMA, we observed increased λ_{\perp} values in the CST, SLF, TRs, and corpus callosum (Table 4).

Figure 2 shows the diffusion indices in the left sensory STR in neonates with no WMA, mild WMA, and moderate WMA.

Discussion

In this structural MR imaging study, we demonstrated important associations between WMA on conventional MR imaging and microstructural changes in specific fiber tracts by using DTI and probabilistic tractography. Compared with neonates with no WMA, those with mild WMA had significantly increased λ_{\perp} and MD values in the left ATR, the left sensory STR, the bilateral motor STR, and for λ_{\perp} also in the right CST; FA decreased significantly in the left sensory STR. Diminished tract volumes and altered diffusion indices were also present in the 2 patients with moderate WMA.

The findings of microstructural changes in specific fiber tracts are consistent with previous DTI studies on predefined ROIs in white matter tissues. WMA were found to be related to changed diffusion indices, in particular to the λ_{\perp} in sensorimotor regions.¹³⁻¹⁵ The increased λ_{\perp} values imply reduced oligodendroglial integrity around the axons.¹² At term-equivalent time, few WM fibers have completely myelinated. In this “premyelinated” stage, pre-OL start to ensheath the axons. The pre-OL are especially vulnerable due to dynamic develop-

ment during the last trimester of pregnancy, and the loss of pre-OL is the most common injury to the preterm brain.³²⁻³⁶ The decrease of pre-OL is counteracted by an increase in oligodendroglial progenitors, shown in several animal models^{37,38}; however, these cells might not have the capacity to further differentiate to become mature myelin-producing cells. Therefore, the altered diffusion indices in this study may relate to the disruption of pre-OL development, which leads to a failure of pre-OL ensheathment of axons. No significant association found in $\lambda_{//}$ suggests that disrupted premyelinating oligodendroglia is the major correlate with WMA rather than axonal pathology.

In neonates with mild WMA, we found bilaterally decreased FA in the sensory STR that, after adjustment for multiple comparisons, was statistically significant at the left side only (Table 2). Because 3 eigenvalues of water diffusion decrease together in the premyelinated period, FA values could have no significant changes in the premyelinated stage.³⁹ In general, myelination starts from posterior to anterior and sensory pathways myelinate before motor pathways⁴⁰; therefore, the altered FA values could emerge earlier in the sensory pathways.

Specific white matter fibers contribute to brain functional networks as information transmitters. The CST and STR are the sensorimotor-related fibers. The CST originates from the frontal cortex, but most fibers come from primary motor and premotor areas, containing mostly motor axons.⁴¹ The STR projects from the ventrolateral nuclei to the frontoparietal cortex, mainly including the motor and somatosensory cortex.^{24,42} The ATR is the projection connecting the frontal cortex and the thalamus; the frontal cortex is considered to play an important role in cognitive and executive functions.⁴³ In our study, preterm neonates with mild WMA compared with no WMA had altered diffusion indices in the CST, STR, and ATR, but not in other fibers. It is possible that the microstruc-

tural changes in those fiber tracts might be responsible for later neurodevelopmental deficits in motor and cognitive functions. In forthcoming studies, these tracts could be selectively studied and correlated with possible neurodevelopmental outcomes in patients with mild WMA at term-equivalent age.

Beyond the microstructural association, no significant differences were found in tract volumes between neonates with no WMA and mild WMA, and only 1 neonate with moderate WMA had some relatively decreased tract volumes. This might suggest that tract volumes were not significantly associated with the subtle WMA.

These findings in tract volumes and diffusion indices are only partly in agreement with the results of de Bruïne et al,¹⁶ who studied fiber tracts in very preterm infants by tractography and found no association between tract lengths and the degree of white matter injury. Our results were different from their findings at the microstructural level: They showed a strong association between DTI indices and the gestational age at MR imaging, but those DTI values were independent of WMA. These different results in diffusion indices might be due to the wide range of gestational age when infants underwent MR imaging because some of their infants were imaged after 46 weeks. Gestational age at MR imaging plays an important role in the changes of diffusion indices,⁴⁴ especially in the first year of life.⁴⁵ In our study, there was no significant difference in the gestational age at MR imaging between groups; however, the gestational age at MR imaging was considered as a covariate when we performed the comparisons.

We evaluated WMA on conventional MR imaging according to the scores of Woodward et al,¹¹ because they studied a large population (167 infants) and included the neurodevelopmental outcome at 2 years of age (corrected for prematurity). Moreover, in our study, we used a careful approach of evaluation to define the degree of abnormalities in 5 characteristics because it was based on a subjective reading. The conventional MR imaging was first evaluated by 2 readers blindly. Second, a consensus was required for the inconsistent categorized cases as well as for the consistent categorized cases with different scores in >2 characteristics. Two cases were excluded due to unresolved discrepancies at consensus. We had a cohort of 70 preterm neonates, but only 2 of them (3%) were classified into the moderate group and there was no neonate with severe WMA, which was less than the amount in other studies with the same classification.^{11,15} However, those studies included very preterm neonates (born at <30 weeks), so those infants might be more sensitive to the effects of extreme prematurity, like greater risks of mortality and morbidity.¹ Another limitation of the present study was that we did not perform DTI and tractography in healthy term neonates, so we were not able to compare our preterm neonates with healthy term neonates.

Conclusions

Altered DTI indices in the CST, STR, and ATR, with λ_{\perp} as the most prominent, were associated with mild WMA on conventional MR imaging in preterm neonates at term-equivalent age.

Acknowledgments

We thank Doni Tamblin for her assistance in language editing.

References

- Slattery MM, Morrison JJ. **Preterm delivery.** *Lancet* 2002;360:1489–97
- van Haastert IC, Groenendaal F, Uiterwaal CS, et al. **Decreasing incidence and severity of cerebral palsy in prematurely born children.** *J Pediatr* 2011;159:86–91
- Fazzi E, Orcesi S, Caffi L, et al. **Neurodevelopmental outcome at 5–7 years in preterm infants with periventricular leukomalacia.** *Neuropediatrics* 1994;25:134–39
- Ohgi S, Akiyama T, Fukuda M. **Neurobehavioural profile of low-birthweight infants with cystic periventricular leukomalacia.** *Dev Med Child Neurol* 2005;47:221–28
- Ramenghi LA, Rutherford M, Fumagalli M, et al. **Neonatal neuroimaging: going beyond the pictures.** *Early Hum Dev* 2009;85:S75–77
- Holsti L, Grunau RV, Whitfield MF. **Developmental coordination disorder in extremely low birth weight children at nine years.** *J Dev Behav Pediatr* 2002;23:9–15
- Taylor HG, Minich NM, Klein N, et al. **Longitudinal outcomes of very low birth weight: neuropsychological findings.** *J Int Neuropsychol Soc* 2004 10:149–63
- Dyett LE, Kennea N, Counsell SJ, et al. **Natural history of brain lesions in extremely preterm infants studied with serial magnetic resonance imaging from birth and neurodevelopmental assessment.** *Pediatrics* 2006;118:536–48
- Inder TE, Wells SJ, Mogridge NB, et al. **Defining the nature of the cerebral abnormalities in the premature infant: a qualitative magnetic resonance imaging study.** *J Pediatr* 2003;143:171–79
- Maalouf EF, Duggan PJ, Rutherford MA, et al. **Magnetic resonance imaging of the brain in a cohort of extremely preterm infants.** *J Pediatr* 1999;135:351–57
- Woodward LJ, Anderson PJ, Austin NC, et al. **Neonatal MRI to predict neurodevelopmental outcomes in preterm infants.** *N Engl J Med* 2006;17:727–29
- Song SK, Sun SW, Ramsbottom MJ, et al. **Dysmyelination revealed through MRI as increased radial (but unchanged axial) diffusion of water.** *Neuroimage* 2002;17:1429–36
- Cheong JL, Thompson DK, Wang HX, et al. **Abnormal white matter signal on MR imaging is related to abnormal tissue microstructure.** *AJNR Am J Neuroradiol* 2009;30:623–28
- Counsell SJ, Shen Y, Boardman JP, et al. **Axial and radial diffusivity in preterm infants who have diffuse white matter changes on magnetic resonance imaging at term-equivalent age.** *Pediatrics* 2006;117:376–86
- Skiöld B, Horsch S, Hallberg B, et al. **White matter changes in extremely preterm infants: a population-based diffusion tensor imaging study.** *Acta Paediatr* 2010;99:842–49
- de Bruïne FT, van Wezel-Meijler G, Leijser LM, et al. **Tractography of developing white matter of the internal capsule and corpus callosum in very preterm infants.** *Eur Radiol* 2011;21:538–47
- Thompson DK, Inder TE, Faggian N, et al. **Characterization of the corpus callosum in very preterm and full-term infants utilizing MRI.** *Neuroimage* 2011;15:479–90
- Hoon AH, Stashinko EE, Nagae LM, et al. **Sensory and motor deficits in children with cerebral palsy born preterm correlate with diffusion tensor imaging abnormalities in thalamocortical pathways.** *Dev Med Child Neurol* 2009;51:697–704
- Counsell SJ, Dyett LE, Larkman DJ, et al. **Thalamo-cortical connectivity in children born preterm mapped using probabilistic magnetic resonance tractography.** *Neuroimage* 2007;34:896–904
- Thomas B, Eyssen M, Peeters R, et al. **Quantitative diffusion tensor imaging in cerebral palsy due to periventricular white matter injury.** *Brain* 2005;128:2562–77
- Evans WA. **An encephalographic ratio for estimating ventricular enlargement and cerebral atrophy.** *Arch Neurol Psychiatry* 1942;47:931–37
- Smith SM, Jenkinson M, Woolrich MW, et al. **Advances in functional and structural MR image analysis and implementation as FSL.** *Neuroimage* 2004; 2(suppl 1):S208–19
- Bassi L, Ricci D, Volzone A, et al. **Probabilistic diffusion tractography of the optic radiations and visual function in preterm infants at term-equivalent age.** *Brain* 2008;131:573–82
- Behrens TE, Johansen-Berg H, Woolrich MW, et al. **Non-invasive mapping of connections between human thalamus and cortex using diffusion imaging.** *Nat Neurosci* 2003;6:750–57
- Johansen-Berg H, Behrens T. *Diffusion MRI.* London, UK: Elsevier; 2009:333–52, 434–36
- Wakana S, Caprihan A, Panzenboeck MM, et al. **Reproducibility of quantitative tractography methods applied to cerebral white matter.** *Neuroimage* 2007;36:630–44
- Liu Y, Balériaux D, Kavcic M, et al. **Structural asymmetries in motor and lan-**

- guage networks in a population of healthy preterm neonates at term-equivalent age: a diffusion tensor imaging and probabilistic tractography study. *Neuroimage* 2010;51:783–88
28. Makris N, Kennedy DN, McInerney S, et al. **Segmentation of subcomponents within the superior longitudinal fascicle in humans: a quantitative, in vivo, DT-MRI study.** *Cereb Cortex* 2005;15:854–69
 29. Aeby A, Liu Y, De Tiege X, et al. **Maturation of thalamic radiations between 34 and 41 weeks gestation: a combined voxel-based study and probabilistic tractography using diffusion tensor imaging.** *AJNR Am J Neuroradiol* 2009;30:1780–86
 30. Powell HW, Parker GJ, Alexander DC, et al. **Hemispheric asymmetries in language-related pathways: a combined functional MRI and tractography study.** *Neuroimage* 2006;32:388–99
 31. Benjamini Y, Hochberg Y. **Controlling the false discovery rate: a practical and powerful approach to multiple testing.** *J R Statist Soc B* 1995;57:289–300
 32. Khwaja O, Volpe JJ. **Pathogenesis of cerebral white matter injury of prematurity.** *Arch Dis Child Fetal Neonatal Ed* 2008;93:153–61
 33. Volpe J. *Neurology of the Newborn.* Philadelphia: W.B. Saunders; 2008
 34. Volpe JJ. **Brain injury in premature infants: a complex amalgam of destructive and developmental disturbances.** *Lancet Neurol* 2009;8:110–24
 35. Back SA, Luo NL, Borenstein NS, et al. **Late oligodendrocyte progenitors coincide with the developmental window of vulnerability for human perinatal white matter injury.** *J Neurosci* 2001;21:1302–12
 36. Haynes RL, Folkerth RD, Keefe RJ, et al. **Nitrosative and oxidative injury to premyelinating oligodendrocytes in periventricular leukomalacia.** *J Neuro-path Exp Neurol* 2003;62:441–50
 37. Yang Z, Covey MV, Bitel CL, et al. **Sustained neocortical neurogenesis after neonatal hypoxic/ischemic injury.** *Ann Neurol* 2007;61:199–208
 38. Sizonenko SV, Camm EJ, Dayer A, et al. **Glial responses to neonatal hypoxic-ischemic injury in the rat cerebral cortex.** *Int J Dev Neurosci* 2008;26:37–45
 39. Dubois J, Dehaene-Lambertz G, Perrin M, et al. **Asynchrony of the early maturation of white matter bundles in healthy infants: quantitative landmarks revealed non-invasively by diffusion tensor imaging.** *Hum Brain Mapp* 2008;29:14–27
 40. Kinney HC, Armstrong DL. **Perinatal neuropathology.** In: Graham DI, Lantos PE, eds. *Greenfield's Neuropathology.* London, UK: Arnold; 2002:557–59
 41. Davidoff RA. **The pyramidal tract.** *Neurology* 1990;40:332–39
 42. Passingham RE, Stephan KE, Kötter R. **The anatomical basis of functional localization in the cortex.** *Nat Rev Neurosci* 2002;3:606–16
 43. Anderson V, Jacobs R, Harvey AS. **Prefrontal lesions and attentional skills in childhood.** *J Int Neuropsychol Soc* 2005;11:817–31
 44. Hüppi PS, Dubois J **Diffusion tensor imaging of brain development.** *Semin Fetal Neonatal Med* 2006;11:489–97
 45. Forbes KP, Pipe JG, Bird CR. **Changes in brain water diffusion during the 1st year of life.** *Radiology* 2002;222:405–09